Ground States and Thermal States of the Random Field Ising Model

Yong Wu and Jonathan Machta

Department of Physics, University of Massachusetts, Amherst, Massachusetts 01003, USA

(Received 28 January 2005; published 23 September 2005)

The random field Ising model is studied numerically at both zero and positive temperature. Ground states are mapped out in a region of random field and external field strength. Thermal states and thermodynamic properties are obtained for all temperatures using the Wang-Landau algorithm. The specific heat and susceptibility typically display sharp peaks in the critical region for large systems and strong disorder. These sharp peaks result from large domains flipping. For a given realization of disorder, ground states and thermal states near the critical line are found to be strongly correlated—a concrete manifestation of the zero temperature fixed point scenario.

DOI: 10.1103/PhysRevLett.95.137208 PACS numbers: 75.10.Nr, 05.70.Fh, 75.10.Hk

The random field Ising model (RFIM) is one of the simplest nontrivial spin models with quenched disorder. Despite 30 years of study it is still not well understood. It has been proved that an ordered phase exists for sufficiently low temperature and dimension $d > 2$ [1–4]. The phase transition between the ordered and disordered phases for $d > 2$ is believed to be continuous and controlled by a zero temperature fixed point [5–7]. Currently, there is no controlled renormalization group analysis of the RFIM phase transition, and Monte Carlo simulations [8–11] are restricted to small systems and have been inconclusive. As the strength of the random field increases, the transition moves to lower temperature and the critical line intersects the zero temperature line at a zero temperature phase transition. Numerical studies of the zero temperature transition [12–15] play an important role in understanding the model. Ground states are much easier to simulate than thermal states and, according to the zero temperature fixed point hypothesis, the $T = 0$ and $T > 0$ transitions are in the same universality class. Critical exponents have been obtained from zero temperature studies that are mostly consistent with the scaling theories [5–7], series methods [16], and real space renormalization group approaches [17–19].

In this Letter we present numerical results at both $T = 0$ and $T > 0$ for the same realizations of random fields. For $T > 0$ we use the Wang-Landau [20] and Metropolis algorithms. For $T = 0$ we find ground states using the push-relabel algorithm [12,21]. A major conclusion of the Letter is that spin configurations found near the critical line are strongly correlated with ground states near the zero temperature critical point. This observation is consistent with the original Imry-Ma analysis, incorporated in the zero temperature fixed point scenario, that the large scale properties of the critical point depend on the competition between random fields and couplings with thermal fluctuations serving only to renormalize the strength of these couplings. However, the correlation found here for single realizations of disorder along the critical line is not implied by the existence of a zero temperature fixed point, which implies only the similarity of zero temperature and positive temperature critical *ensembles.*

The Hamiltonian of the RFIM studied in this Letter is

$$\mathcal{H} = -\sum_{\langle i,j\rangle} s_i s_j - \Delta \sum_i h_i s_i - H \sum_i s_i. \qquad (1)$$

The summation $\langle i, j\rangle$ is over all nearest neighbors i and j on a simple cubic lattice with periodic boundary conditions, spins s_i take the value ± 1, Δ is the strength of disorder, h_i is the random field chosen from a Gaussian distribution with mean zero and variance one, and H is the external field. Two important quantities are the magnetization (order parameter) $m = (1/L^3)\sum_i s_i$ and the bond energy $e = (1/L^3)\sum_{\langle i,j\rangle} s_i s_j$. We define the disorder strength separately from the normalized random fields because one of our primary concerns is to examine single realizations of random fields as disorder strength, temperature and external field are varied. Previous analytic [22] and real space renormalization group studies [17] also considered single realizations of disorder at the phase transition but do not

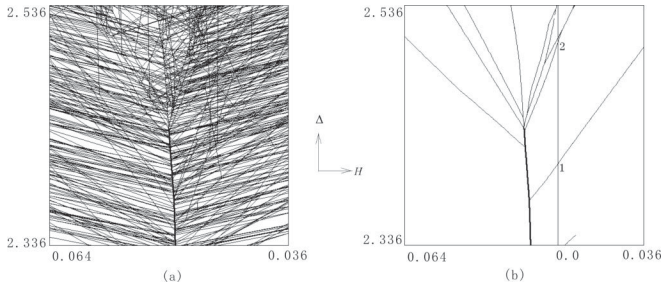

FIG. 1. Ground states of the RFIM in the H-Δ plane. (a) All the ground states of a single 32^3 realization of disorder. Along each line two ground states coexist that differ by flipping a single connected domain. The thickness of a line is proportional to the magnetization jump across the line. (b) The same realization as in (a), but only lines with the bond energy jump $\delta e > 0.03$ are shown. Along the $H = 0$ axis there are two major jumps, which are labeled as 1 and 2 in the graph.

compare realizations at different disorder strengths as is done here.

Consider the set of ground states of a single realization of disorder. We obtain these using a method first introduced by Ogielski [12]. To determine the ground state at a given value of H and Δ, the RFIM problem is mapped onto the maxflow problem, which is then solved using the push-relabel algorithm [12,21,23,24]. The set of all ground states in a region in the H-Δ plane is mapped out using a method described in [25] and similar to the techniques discussed in [15,26]. Figure 1(a) is a portrait of all the ground states of a single realization of random fields in a 32^3 system in a small region of the H-Δ plane near the finite-size critical point, discussed below. Each line represents values of the parameters for which two ground states are degenerate and across each line a single connected domain is flipped. Within each polygon bounded by these lines, a single spin configuration is the ground state. At points where two lines cross, four ground states are degenerate and the four configurations differ by the orientation of two separate domains. More interesting are ''triple points'' where a line bifurcates into two lines in a Y shape. At triple points three ground states are degenerate, but the three domains corresponding to the three lines are not independent. The spin configuration at the top of the Y results from the breakup of the large domain that flips across the vertical line of the Y as shown schematically in Fig. 2. The triple point has some characteristics of a thermal first-order transition where two ordered states coexist with a disordered state.

When a coexistence line is crossed and a domain is flipped, physical quantities except for the total energy are discontinuous. To visualize the size of the discontinuity, lines are drawn with a thickness that is proportional to the jump in the magnetization. The picture is simplified by removing the large number of lines with small bond energy jump ($\delta e < 0.3$), as shown in Fig. 1(b). The simplified picture reveals a treelike structure built from triple points. The triple point with the largest bond energy discontinuity is located at the center of the picture. In the region above this triple point the magnetization is small while the line extending below the triple point is the coexistence line separating the plus and minus ordered states. In Ref. [15] this triple point was identified as the finite-size critical point and its scaling properties were studied. The size of the discontinuity in the bond energy is governed by the specific heat exponent. We have also examined the large discontinuities in bond energy and magnetization along the $H = 0$ line and have shown [25] that these scale with the specific heat exponent and magnetic exponents, respectively. Within a region that shrinks as $L^{(\alpha+\beta-2/)\nu}$ and $L^{1/\nu}$ in the H and Δ directions, respectively, the treelike structure is statistically self-similar but not self-averaging—each realization has a unique treelike structure.

We study the RFIM as a function of temperature using the Wang-Landau [20] and the Metropolis algorithms. The Wang-Landau algorithm is a flat histogram Monte Carlo method that automatically determines the density of states.

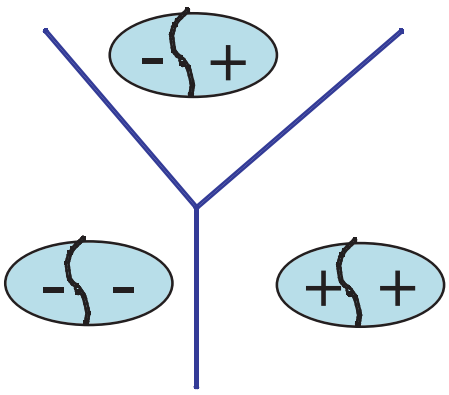

FIG. 2 (color online). Schematic picture of a triple point. The shaded ovals show the orientation of spins within a single domain that flips crossing the vertical line and is broken into two pieces crossing the diagonal lines.

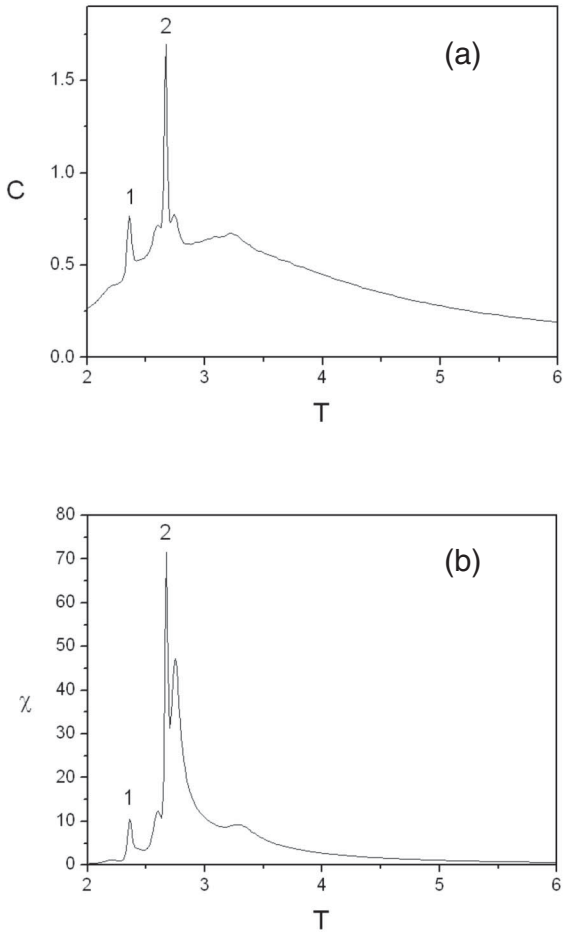

FIG. 3. The specific heat (a) and the susceptibility (b) of the same 32^3 realization as in Fig. 1 with $\Delta = 2.0$ and $H = 0$. Two sharp peaks, labeled 1 and 2, are observed, which correspond to the two large jumps 1 and 2 in Fig. 1, respectively.

Thermodynamic quantities at all temperatures are then derived from the density of states and the statistics of the magnetization as a function of energy. The algorithm smooths the energy landscape and is much more efficient than the conventional Metropolis algorithm for sweeping a range of temperatures. Once a temperature is chosen for detailed study, the Metropolis algorithm is used to find the thermally averaged spin configuration. We determined the specific heat and susceptibility for systems up to size 32^3. We find that for large enough systems ($\geq 16^3$) and strong enough disorder, the specific heat and the susceptibility typically display one or more sharp peaks. In Fig. 3 we show the specific heat and the susceptibility as a function of temperature for the same realization of normalized random fields whose ground states are shown in Fig. 1. The random field strength is $\Delta_0 = 2.0$ and the external field is set to zero. Two sharp peaks appear in both quantities at the same temperatures. We have simulated 100 16^3 realizations with $\Delta_0 = 1.5$ and find that about $1/3$ of them have sharp peaks. The number increases to $1/2$ if the random field is strengthened to $\Delta_0 = 2.0$. For size 32^3 and $\Delta_0 = 2.0$ we have simulated 9 realizations, and sharp peaks are observed for all of them. We tentatively conclude that the probability of sharp peaks appearing increases with the system size and the strength of random field.

The sharp peaks in the specific heat and susceptibility can be understood within the zero temperature fixed point picture of the RFIM phase transition. This picture predicts that the behavior in the critical region at finite temperature is determined by the competition between couplings and random fields with thermal fluctuations serving only to renormalize the strength of these quantities. One conclusion of this Letter is that this scenario appears to be true for individual realizations of normalized random fields. The sharp peaks in the thermodynamic quantities can be matched one to one with the large jumps at zero temperature. Furthermore, the spin configurations on either side of the sharp peaks can be mapped onto the ground states on either side of the corresponding large jumps.

For a single realization of random fields, we obtain the thermally averaged spin configuration near the peaks at finite temperature, and compare these thermal states to the ground states near the two largest jumps at zero temperature. Figures 4(d)–4(f) show one plane through the system with $\Delta_0 = 2.0$ and at temperatures just before peak 1 ($T = 2.2$), just after peak 1 ($T = 2.5$), and just after peak 2 ($T = 2.8$), respectively. The difference among the states shows that the sharp peak corresponds to flipping a relatively large domain. It is evident that these three states are strongly correlated with the ground state spin configuration before jump 1 ($\Delta = 2.36$), just after jump 1 ($\Delta = 2.41$), and just after jump 2 ($\Delta = 2.54$), as shown in Figs. 4(a)–4(c), respectively. [The labels of jumps and peaks are given

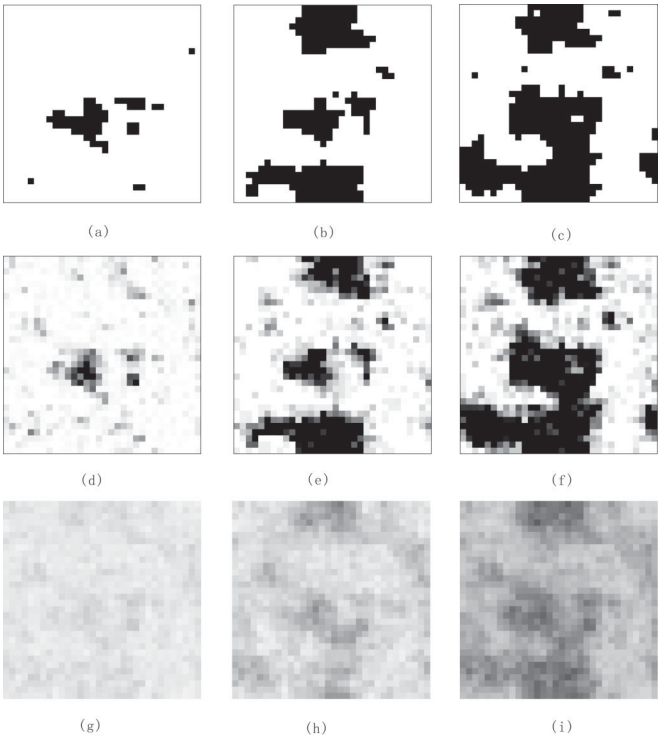

FIG. 4. Spin configurations near the critical points at zero temperature and finite temperatures for a single realization of normalized random fields. Each panel is the same plane of a 32^3 realization with black representing spin down; white, spin up; and shades of gray, the thermally averaged spin state. From left to right in the top two rows, panels are at Δ (T) before, between, and after jumps (peaks) 1 and 2 in Fig. 1 (Fig. 3). Specifically, panels (a), (b), and (c) are ground states at $\Delta = 2.36$, 2.41, and 2.54, respectively. Panels (d), (e), and (f) are at $\Delta = 2.0$ and $T = 2.2$, 2.5, and 2.8, respectively. Panels (g), (h), and (i) are at $\Delta = 0.5$ and temperatures 4.0, 4.3, and 4.45, near the peak in the specific heat at $T = 4.375$.

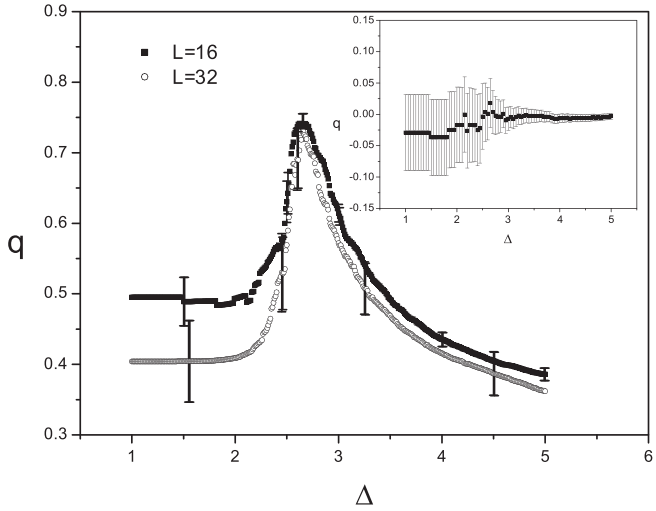

FIG. 5. Disorder averaged correlation q of a thermal state just above the transition temperature at $\Delta_0 = 1.5$ to ground states at disorder strength Δ for the same realization of random fields. Solid squares for size 16^3 and open circles for size 32^3. Only a few error bars are drawn to make the figure easy to read. The inset shows the correlation of thermal states with ground states of a different random field realization.

in Figs. 1(b) and 3.] Similar correlations between ground states and thermal states were found in one dimension [27].

Some correlation between ground states and thermal states persists to much smaller values of Δ_0 in a regime where the thermodynamic properties no longer display sharp peaks. Figures 4(g)–4(i) show the same realization of disorder and the same plane through the system but with $\Delta_0 = 0.5$. Here the specific heat has a rounded peak at $T = 4.375$. Figures 4(g)–4(i) correspond to temperatures 4.0, 4.3, and 4.45, respectively. Although there is considerable thermal "blurring" in these pictures, evidence of the ground state is unmistakable.

A quantitative characterization of the correlation between ground states and thermal states for the same realization can be obtained from the correlation measure,

$$q(\Delta) = \frac{1}{L^3} \sum_i \overline{\mathrm{sgn}(\langle s_i \rangle_{\Delta,0} \langle s_i \rangle_{\Delta_0,T^*})}, \qquad (2)$$

where the overbar is an average over realizations of disorder and $\langle s_i \rangle_{\Delta,T}$ is the thermal average of the spin at the ith site at disorder Δ and temperature T or, if $T = 0$, it is the ground state spin value. For each realization, the temperature $T^* = T_{\max} + 0.1$ where $T_{\max}$ is the temperature of the maximum of the specific heat or one of the sharp peaks in C if sharp peaks exist. Thus, for each realization, we pick a thermal state just above the transition temperature. Figure 5 shows q vs Δ for sizes 16^3 and 32^3 and $\Delta_0 = 1.5$, with 96 realizations for size 16^3 and 9 for size 32^3. A peak in the correlation occurs at $\Delta \approx 2.65$ where $q \approx 0.75$. The value, $\Delta \approx 2.65$, is about 0.15 larger than the average Δ at the largest discontinuity in the bond energy for system size 32^3. The inset of Fig. 5 shows the average correlation between thermal states of one realization and ground states of another for size 16^3, which is nearly zero as expected. A second measure q^* is obtained by choosing the value Δ^* for each ground state realization to give the largest correlation to the thermal state at T and then averaging over realizations. We find that, for size 32^3, $q^* = 0.80 \pm 0.06$ for $\Delta_0 = 1.5$ and $q^* = 0.85 \pm 0.05$ for $\Delta_0 = 2.0$. Together, these results provide quantitative confirmation that the thermal states at temperatures slightly above the thermal critical point are strongly correlated with the ground states at disorder strength slightly higher than the zero temperature critical point.

The strong correlations between states at different temperatures are ostensibly in conflict with the idea of "chaos" in the RFIM. Chaos in systems with quenched disorder, such as spin glasses and the RFIM, refers to the sensitivity of spin configurations to small perturbations either in temperature or in quenched disorder [14,28,29]. The existence of chaos in the RFIM is controversial and is not definitively established. This work suggests that chaos is not present along trajectories in the Δ-T plane following the critical line.

In summary, we find that sharp peaks in thermodynamic functions resulting from the flipping large domains are typical near the critical point. In addition, spin configurations near the transition are similar to the ground states near some corresponding large jump at zero temperature. If this connection between critical ground states and thermal states persists to large system size, it supports a strong version of the zero temperature fixed point scenario: the sequence of states near the zero temperature critical point obtained by varying Δ for $T = 0$ can be mapped onto the sequence of thermal states near the critical point obtained by varying T for fixed values of Δ_0, $\Delta_0 < \Delta_c$.

We thank Alan Middleton and Moshe Schwartz for useful discussions. This work was supported by NSF Grant No. DMR-0242402.

[1] Y. Imry and S. K. Ma, Phys. Rev. Lett. **35**, 1399 (1975).
[2] G. Grinstein and S. K. Ma, Phys. Rev. Lett. **49**, 685 (1982).
[3] J. Z. Imbrie, Phys. Rev. Lett. **53**, 1747 (1984).
[4] J. Bricmont and A. Kupiainen, Phys. Rev. Lett. **59**, 1829 (1987).
[5] A. J. Bray and M. A. Moore, J. Phys. C **18**, L927 (1985).
[6] J. Villain, J. Phys. (Paris) **46**, 1843 (1985).
[7] D. S. Fisher, Phys. Rev. Lett. **56**, 416 (1986).
[8] H. Rieger and A. P. Young, J. Phys. A **26**, 5279 (1993).
[9] H. Rieger, Phys. Rev. B **52**, 6659 (1995).
[10] M. E. J. Newman and G. T. Barkema, Phys. Rev. E **53**, 393 (1996).
[11] J. Machta, M. E. J. Newman, and L. B. Chayes, Phys. Rev. E **62**, 8782 (2000).
[12] A. T. Ogielski, Phys. Rev. Lett. **57**, 1251 (1986).
[13] A. K. Hartmann and A. P. Young, Phys. Rev. B **64**, 214419 (2001).
[14] A. A. Middleton and D. S. Fisher, Phys. Rev. B **65**, 134411 (2002).
[15] I. Dukovski and J. Machta, Phys. Rev. B **67**, 014413 (2003).
[16] A. Gofman, J. Adler, A. Aharony, A. B. Harris, and M. Schwartz, Phys. Rev. Lett. **71**, 2841 (1993).
[17] M. Gofman, I. Dayan, M. Schwartz, and A. P. Young, J. Phys. A **26**, 3093 (1993).
[18] M. S. Cao and J. Machta, Phys. Rev. B **48**, 3177 (1993).
[19] A. Falicov, A. N. Berker, and S. R. McKay, Phys. Rev. B **51**, 8266 (1995).
[20] F. Wang and D. P. Landau, Phys. Rev. E **64**, 056101 (2001).
[21] A. V. Goldberg and R. E. Tarjan, J. ACM **35**, 921 (1988).
[22] M. Schwartz and A. Soffer, Phys. Rev. B **33**, 2059 (1986).
[23] B. Cherkassky and A. V. Goldberg, Algorithmica **19**, 390 (1997).
[24] The algorithm is available from Andrew Goldberg's Network Optimization Library, http://www.avglab.com/andrew/soft.html.
[25] Y. Wu and J. Machta (to be published).
[26] C. Frontera, J. Goicoechea, J. Ortín, and E. Vives, J. Comput. Phys. **160**, 117 (2000).
[27] G. Schröder, T. Knetter, M. J. Alava, and H. Rieger, Eur. Phys. J. B **24**, 101 (2001).
[28] A. J. Bray and M. A. Moore, Phys. Rev. Lett. **58**, 57 (1987).
[29] M. Alava and H. Rieger, Phys. Rev. E **58**, 4284 (1998).